Computational and Theoretical Chemistry 1016 (2013) 36–41

Contents lists available at SciVerse ScienceDirect

Computational and Theoretical Chemistry

journal homepage: www.elsevier.com/locate/comptc

Theoretical description of benzene–fullerene and its organometallic derivative

Anabel Ruiz-Espinoza, Estrella Ramos, Roberto Salcedo *

Instituto de Investigaciones en Materiales, Universidad Nacional Autónoma de México, Circuito Exterior s/n, Ciudad Universitaria, Coyoacán 04510, Mexico City, Mexico

ARTICLE INFO

Article history:
Received 15 November 2012
Received in revised form 10 April 2013
Accepted 11 April 2013
Available online 21 April 2013

Keywords:
Benzene–fullerene
Aromaticity
Organic derivatives
Organometallic derivative

ABSTRACT

The ubiquitous benzene derivative of fullerene has been analyzed from a theoretical point of view. The pronounced difficulties involved in its preparation relate to the structure of the frontier orbitals of the primitive fragments (i.e. benzene and fullerene C_{60}) and their corresponding interactions. The nature of the inductive effect is studied on the basis of the nitro and amino derivatives (functional groups substituted on benzene ring). The electrophilic activation/deactivation patterns induced by substituent groups added to phenyl-fullerene molecule are studied applying the criteria of reactivity indexes in conjunction with the molecular electrostatic potential and the dipole moment of the molecules. The capacity of the resultant molecule to generate organometallic derivatives similar to the dibenzene-chromium is also studied. All structures were calculated using DFT methods.

1. Introduction

The organo-fullerene compounds comprise a rare classification of substances because the direct reactions between fullerene and organic fragments are not common [1]. There are several methods which can be used to synthesize the so-called organohydrofullerenes where a double bond on the fullerene surface is broken to yield the substitution of a functional group and a hydrogen atom [2]. Among these, it is important to mention those compounds where the substitution makes it possible for an aromatic ring to take a substituent on one end of a double bond, and a hydrogen atom on the other [3,4], causing an elecrophilic aromatic substitution to occur. This type of compound constitutes the subject of our interest.

The phenyl-fullerene (**PF**) is presented in Fig. 1; the molecule is the only product resulting from the substitution of a benzene molecule on a (6,6) fullerene bond and its corresponding proton. The first attempt to prepare this compound was undertaken by Olah and his co-workers [5], but the problem encountered in a direct reaction lies in the possibility that a multiple substitution will take place at the surface of the C_{60}, it is thus convenient that the products should consist of a mix of several substances. The titration method [3,4] has been shown to represent a better option and the phenyl-fullerene can be synthesized in this way, however little information exists concerning its structure and reactivity.

The goal of this study is to analyze the nature of the electronic structure of this molecule from a theoretical point of view, analyzing the intrinsic properties involved in possible reactive behavior, the changes precluded by new substituents on the benzene fragment and the possibility of preparing organometallic derivatives.

2. Methods

All calculations were carried out by applying a pure DFT method for energy evaluations. In the case of structures of all derivatives of benzene, Becke's gradient corrections [6] for exchange and Perdew–Wang's for correlation [7] were applied. This is the scheme for the BPW91 method which forms part of the Gaussian 09 [8] Package. The calculations were performed using the 6-31G** basis set. The structure of complex di-benzenechromium-fullerene (**BCF**) was optimized using DFT in the generalized gradient approximation (GGA) with the Materials Studio DMol3 program [9,10] from Accelrys Inc. We employed the Perdew–Wang 1991 (PW91) exchange–correlation functional [11] with a double numerical, plus a polarization function basis set (DNP) to describe the valence electrons, in combination with Hartree–Fock effective core potentials [12,13] for the treatment of the ionic cores. The structure was relaxed until the total remaining force was below 0.002 Ha/Å, a thermal smearing of 0.05 Ha was used to optimize geometry. Finally, the structure was optimized with Gaussian 09.

Frequency calculations were carried out at the same level of theory in order to confirm that the optimized structures were at a minimum on the potential surfaces. Work strategy was selected according to that proposed in the previous fullerenocene study [11]. The bond lengths of the optimized structures were used for

* Corresponding author. Tel.: +52 5556224600.
E-mail address: salcedo@unam.mx (R. Salcedo).

2210-271X/$ - see front matter © 2013 Elsevier B.V. All rights reserved.
http://dx.doi.org/10.1016/j.comptc.2013.04.011

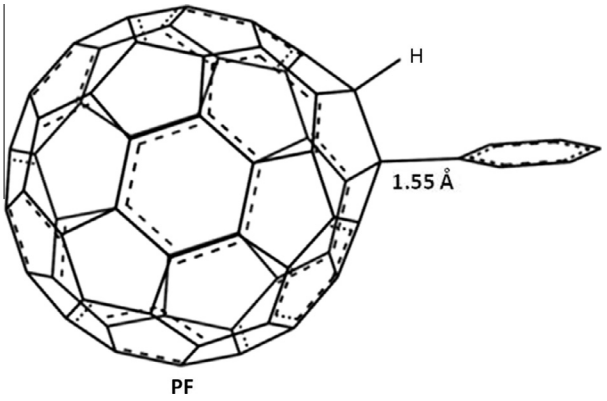

Fig. 1. DFT optimized geometry BPW91/6-31G** of **PF.**

the HOMA (Harmonic Oscillator Model of Aromaticity) method [14,15] for studying aromaticity.

3. Model equations

The global eletrophilicity, ω, defined by Parr et al. [16] as $\omega = \frac{\mu^2}{2\eta}$, is evaluated in terms of the electronic chemical potential μ (the negative of Mulliken electronegativity) approached by $\mu = -\frac{(I+A)}{2}$ and the chemical hardness η defined as $\eta = (I - A)$. They are evaluated in terms of the vertical ionization potential I and electron affinity A for the ground state of the molecules, at the BPW91/6-31G** level of theory. The maximum electron flow ΔN_{max} is given as $\Delta N_{max} = -\frac{\mu}{\eta}$.

4. Results and discussion

The first molecule that was studied is **PF** presented in Fig. 1. The results suggest that the molecule is stable from a thermodynamic point of view; the frequency calculation indicates that there are not imaginary frequency values.

The nature of the **PF** molecule manifests a narrow energy gap (1.47 eV) between the HOMO and LUMO. In the fullerene (**F**) the corresponding value is 2.762 eV previously obtained [17]. This situation arises due to the new arrangement of molecular orbitals (MOs). Originally the molecular orbitals of **F** presented an arrangement portraying a threefold degenerated set for the LUMO and a fivefold degenerate set for the HOMO. In the case of benzene (**B**) it manifests the classic distribution of a twofold degenerate set for the HOMO and a near HOMO-1 which completes the sextet. Mixing both molecules produces a large set of eight delocalized and occupied MOs that are very similar in energy and exert a strong electronic influence, stronger than the one exerted by the fivefold degenerated set of the fullerene. Therefore the LUMO is attracted by this force and the gap in **PF** is lower than it is in a pure **F** molecule. All this is depicted in the interaction diagram presented in Fig. 2.

It is important to note that the energy of the HOMOs in both cases (i.e. **B**: −5.95 eV, **F**: −5.98 eV) is almost the same. It seems possible that an electronic pair originally situated on the HOMO of benzene could transfer to one of the three orbitals of the degenerated set of the fullerene LUMO and meanwhile the other four aromatic electrons from the benzene mix with the fullerene HOMO. Obviously the symmetry of the **PF** is very low and the large degeneration taking place in the parent molecules is lost. However, the new levels are very similar, suggesting electronic flow. The shapes of the molecular orbitals are presented in Fig. 2, all of them demonstrate strong fullerene participation. Indeed, the LUMO only manifests fullerene participation and the HOMO, along with the threefold degenerate set of HOMO-1 orbitals presents little participation of benzene and a bond between both fragments.

This scheme is useful for establishing the reactive nature of **PF**. A very important feature is that the LUMO represents a low energy double degeneracy which can provide the site for easy electrophilic substitution, a characteristic which varies little from that displayed by pristine fullerene which is shown to have a weak electronic acceptor nature. In contrast, **PF** is actually a strong electronic acceptor. The HOMO and HOMO-1 set also play an important role in this discussion because they offer eight electrons for interaction with a very near LUMO. Thus semiconductor behavior is addressed.

The aromaticity of the ring joined to the **F** is expected to change to some extent, so the evaluation of this possible modification was carried out by applying the HOMA method [14,15]. The result is interesting because the predicted value for free **B** is 1.0 and the value obtained for the **B** ring in our case is 0.995, therefore the change is minimal and indicates that the **F** substituent displays almost neutral behavior because the hypothetical reactivity of **B** manifests few changes.

In order to assess the last statement, new calculations were carried out involving various functional groups substituted at the *para* position on the **B** fragment to compare with the substitution on the fullerene sphere. The substituents consisted firstly of an electron releasing agent $-NH_2$ (**APF**) and secondly an electronic withdrawing agent such as the $-NO_2$ group (**NPF**) (Fig. 3). The analysis of these results is presented later in the text.

The electronic gap in the new molecules reflects the expected changes. The energy gap for the nitro substituted molecule is practically the same as that of **PF**; the value is 1.43 eV in comparison with 1.47 eV in the case of the unsubstituted one. The interesting

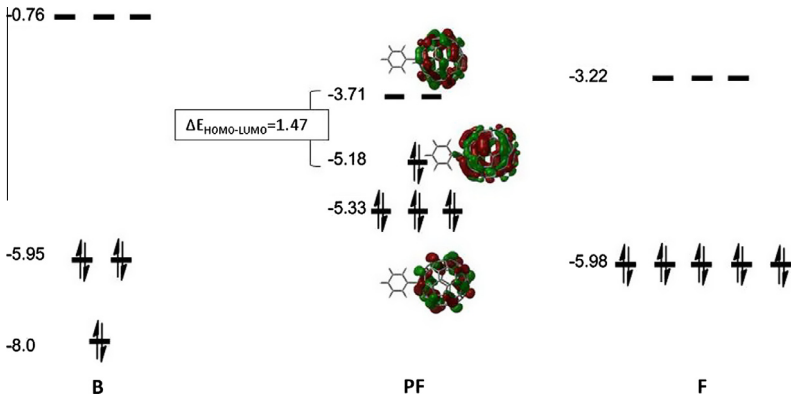

Fig. 2. Interaction molecular orbital diagram sets for **B**, **PF** and **F** (eV).

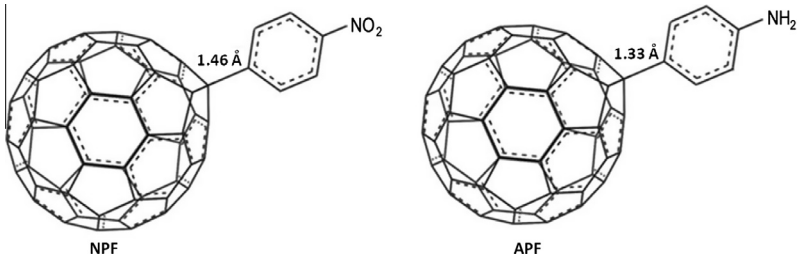

Fig. 3. Nitro and amine derivatives of **PF.**

change comes in the case of the amino substituted species, where the energy gap is 1.3 eV. The inductive effect has impact on the electronic structure. The flow of electrons comes from the substituent to the ring in the case of the $-NH_2$ group. Therefore the LUMO is more strongly attracted in this instance. In contrast, the $-NO_2$ substituted molecule manifests an inverted flow but the electronic structure is similar to the unsubstituted case. The comparative interaction in MOs diagram may be useful for showing these features (see Fig. 4).

There are also important differences in terms of the shapes of the molecular orbitals; those coming from the nitro derivative (**NPF**) have practically the same shape as the corresponding ones in the **PF** molecule. However, in the amino derivative (**APF**) dramatic changes are apparent because the aromatic ring shows important participation at the donor level, which does not occur in the previous cases. The substitution with a $-NH_2$ group contributes to obtain a compound with a shorter band gap. The corresponding molecular orbital diagram shows that a quasi-double fold degenerated set is present in the case of the HOMO, a feature that accounts for the strong attraction on the part of the LUMO. The band gap of the **NPF** compound is larger than the corresponding to **PF**. The effect of the $-NO_2$ group electronegativity provokes a decrease of the HOMO and LUMO energy values with respect to the **PF** compound. The electronic behavior is almost the same, i.e. all three substances should represent promising candidates for semiconductor applications.

On the other hand, the reactivity is also different because in the case of the amino substituted compound the LUMO is more exposed to an electronic attack than in the other instances. Therefore, an electrophilic reaction can occur on it. However, the region of the HOMO should also be reactive because it has four electrons all able to participate in a nucleophilic reaction. Thus, the reactivity for this compound could be more versatile than in the other cases.

Elevated electronic richness is a feature common to all these cases, as a consequence of the original electronic accumulation on the HOMO of pristine **F** that is reflected in the substituted complexes. There is thus a temptation to test the molecule in a model where electrons are able to interact to form new species. A classic example would be the interaction with transition metal atoms. Therefore, an organometallic sandwich was designed. The shape of this organometallic complex is shown in Fig. 5. The original **PF** interacts with a chromium atom and another benzene ring to form a derivative of di-benzenechromium (**BC**).

The semiconductor behavior of this organometallic molecule is once again assessed with reference to the HOMO–LUMO gap. The corresponding value is 0.01 eV. This is a very interesting result because this compound can be considered as a strong conductor or even as a synthetic metal. The interaction diagram of the frontier

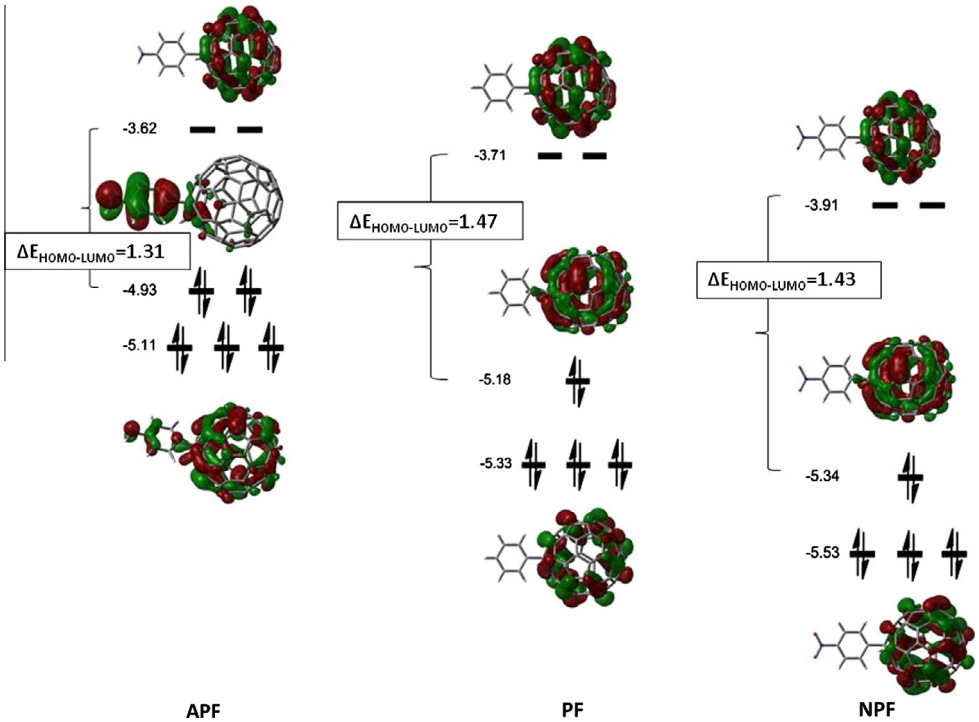

Fig. 4. Diagram of interaction sets for molecular orbitals of **APF**, **PF** and **NPF** (eV).

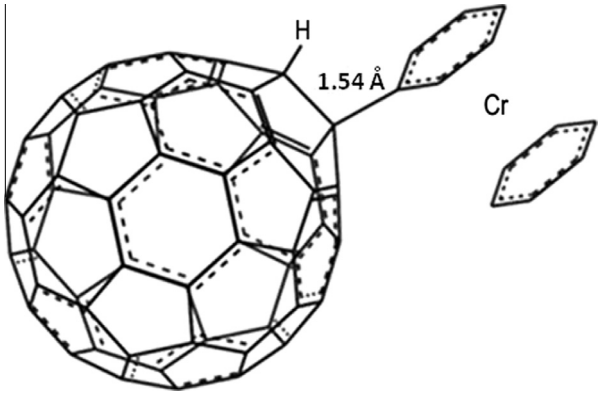

Fig. 5. Di-benzenechromium fullerene (**BCF**).

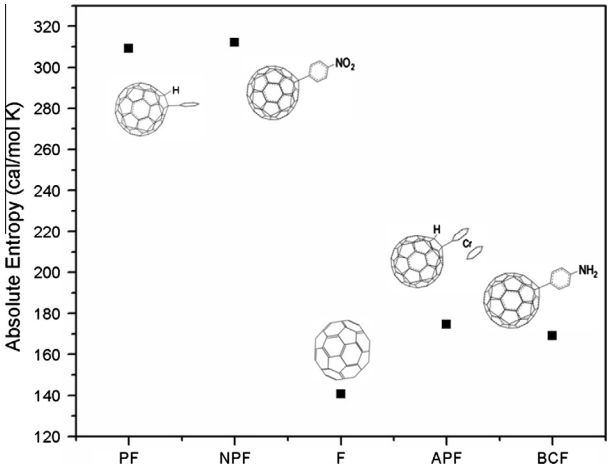

Fig. 7. Absolute entropy for all molecules studied.

molecular orbitals and the shape of these eigenfunctions are presented in Fig. 6.

The curious point in this case is that the HOMO is derived completely from the **BC** fragment, whereas the LUMO is a pure **F** combination. The origin of these eigenfunctions is interesting. Firstly, the HOMO is derived from the e_{2g} molecular orbital of the original HOMO-1 of **BC**. This MO is a combination of d_{xz} and d_{yz} and certain symmetric combinations derived from the aromatic ring, the key point being that the HOMO of the **BC** does not participate in the frontier molecular orbitals of the fullerene complex. This molecular orbital is presented as the HOMO-2 function in the new interaction diagram. Secondly, the LUMO of the fullerene complex is practically an appreciable part of the original LUMO of isolated **F** (t_{1u}). Therefore, the behavior in this complex will involve the participation of the fullerene fragment in electrophilic reactions and participation of the **BC** fragment in nucleophilic reactions, which is the same as the **APF** derivative behavior. This is a very interesting feature in the **BCF** complex because the chemistry varies radically from one case to the other. It is important to note that the **PF** molecule depicted above manifests very different behavior, because in this instance almost all the frontier MO's are focused on the **F** fragment and the aromatic **B** ring participates very little, so that in this instance all reactions must be oriented to the **F**.

The relative stability of each proposed molecule has been estimated considering their absolute entropy values because it is not possible to make a direct comparison of thermodynamic values since this is not a set of isomers. Therefore, the entropy of pristine fullerene calculated at the same level of theory has been considered as a reference. Fig. 7 shows the absolute entropy values of the five species. Obviously, the fullerene entropy has a very low value because it is a very symmetric structure in comparison with the studied molecules, but the relative differences are very significant. It is notorious that the derivatives are found in two groups, the first one contains the **PF** and the nitro derivative **NPF**, which have more or less a similar behavior; in the second one are the aniline **APF** and the organometallic derivatives **BCF** which have the lower entropy values with the exception of pristine fullerene. It is important to note that the only experimentally known species of the studied items is the phenyl-fullerene which shows large absolute entropy. Therefore, it is possible to expect that the other compounds could be prepared.

The inductive effect caused by substitution on a phenyl ring is evident in the analysis of the molecular electrostatic potential of the four different molecules. Fig. 8 shows the molecular electrostatic potential surface for **PF**, **NPF**, **APF** and **BCF**.

Taking the **PF** molecule as a reference, it is possible to observe that the effect of the deactivant group ($-NO_2$) provokes a decrease in electron density upon the **F** fragment. There is an opposite effect of the activant group ($-NH_2$) where the distribution of electron density upon the fullerene fragment increases with respect to the **PF** molecule. With respect to the **BCF** molecule, the behavior is analogous to the **APF** substituted molecule. This was a test to define whether the **BC** fragment has an electron-releasing nature, which appears to be the case. The magnitude and direction of the dipole moment vector is used as evidence of the asymmetry in

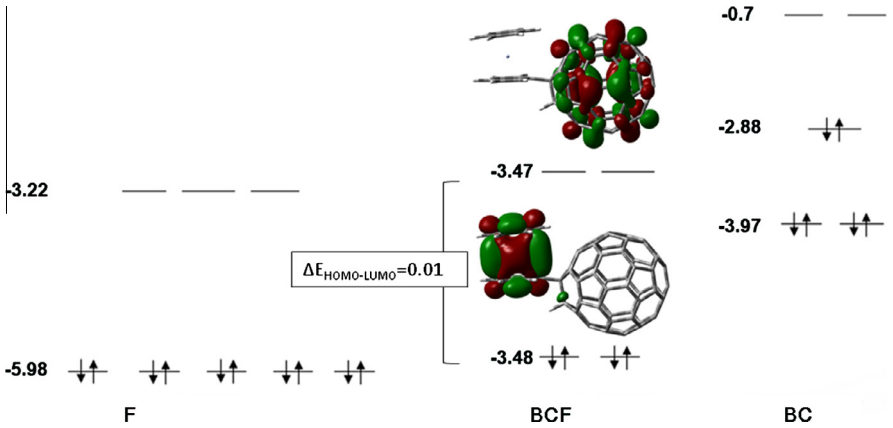

Fig. 6. Diagram of interaction between molecular orbitals and sets of frontier molecular orbitals of **F**, **BCF** and **BC**. Frontier molecular orbitals of the organometallic complex are shown.

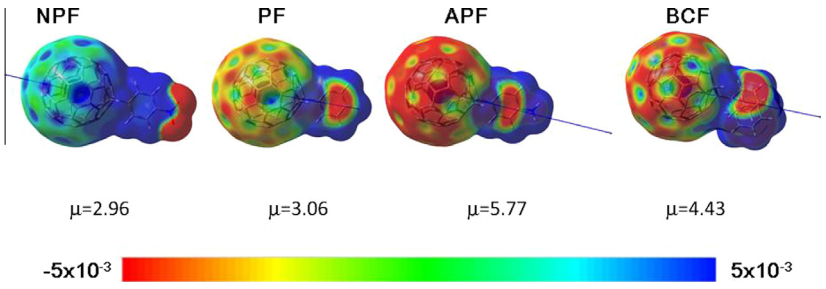

Fig. 8. Molecular electrostatic potential (eV) mapped onto electron density for the four studied systems showing dipole moment vector (D). For clarity, the dipole moment vector is augmented 3 times with respect to their value. All molecules are presented in the same scale.

Table 1
Theoretical reactivity indexes BPW91/6-31G** in atomic units calculated for **PF**, **APF**, **NPF** and **BCF** as described in Section 3.

Molecule	Ionization energy (I)	Electron affinity (A)	Chemical potential (μ)	Molecular hardness (η)	Electron flow (ΔN_{max})	Global electrophilicity (ω)
BCF	0.176	0.084	−0.260	0.093	2.805	0.364
APF	0.237	0.077	−0.314	0.159	1.964	0.308
PF	0.247	0.080	−0.327	0.167	1.957	0.320
NPF	0.255	0.090	−0.345	0.165	2.089	0.359

Considering that **F** acts as the electrophile agent in all these compounds, it is possible to analyze which member of the substituent group causes major electron flow ΔN_{max}. This quantity can be measured by the amount of additional electronic charge needed to stabilize an electrophile. The global electrophilicity represents the susceptibility of the system to acquire an additional amount of electronic charge ΔN_{max}, considering two properties : the first one consists of the chemical potential as a measurement of the tendency of the system to electron diffusion and the second one is the resistance of the system to exchange electronic charge with the environment, which is called chemical hardness [16].

the charge distribution of the molecules. The effect of deactivation caused by the NO_2 group is inferred as a change in the direction of the dipole moment vector with reference to the **PF** molecule.

The analysis of distribution of the molecular electrostatic potential yields some additional information. The electrophilic activation/deactivation patterns induced by substituent groups added to **PF** molecule arise from this analysis. The distribution of the molecular electrostatic potential can be studied together with pure indexes of reactivity arising from the density functional theory developed by Parr et al. [16]. Table 1 shows these theoretical indexes, calculated by applying the chemical model BPW91/6-31G**. The vertical ionization energy (I) and electron affinity (A) are calculated from the energy difference between the cation with respect to the neutral molecule and the neutral with respect to the anion, respectively.

From Table 1, it is possible to make a simple analysis involving only the organic derivatives. In this sense it is apparent that the maximum flow is manifested by the $-NO_2$ substituted molecule. This attribute can be explained by the fact that the **F** fragment in this compound is shown as a region with positive potential (see Fig. 7), indicating that it will accept more negative charge than any other species. Accordingly, it is possible to observe that the **NPF** has a greater ω value than **PF** and **APF**. These results agree with the fact that the **NPF** is the molecule with the lowest LUMO level (see Fig. 4). The electron flow in both **PF** and **APF** is very similar. However, the electrophilicity of **PF** is higher than that of **APF**, which can be explained by means of the distribution of positive potential on all the compounds. The molecular electrostatic potential chart clearly shows a more positive potential in the **NPF** compound, followed by **PF** and, finally, the **APF** constitutes the least electropositive species.

The electrostatic potential distribution, electron flow and electrophilicity of the chromium complex follows the tendency of the $-NH_2$ substituted molecule, where the fullerene fragment is activated due to the charge distribution. The maximum flow of the **BCF** complex represents the greatest value for the entire series and it does manifest the greatest electrophilicity. Fig. 6 shows the shape of the frontier molecular orbitals of the metallic complex, where it is possible to appreciate that there is a net electronic flow from HOMO to LUMO between the **BC** (HOMO) and the **F** (LUMO) fragments. A similar phenomenon is present in the **APF** compound in which there is a strong localization of the fullerene and the aromatic fragment in the HOMO and LUMO without mixing. This kind of flow does not appear in the **PF** species and neither in the **NPF**. However, this phenomenon is not enough to yield a large electrophilicity value since the NO_2 derivative has a higher electrophilicity than **PF** and **APF** and it shows a large value of electronic flow, but it is clear from the Molecular Orbital splitting diagram that this flow is localized completely in the **F** fragment. A global sight of the analysis shows that those compounds containing the aniline and the organometallic substituents have the lower energy gaps between HOMO and LUMO. Also, the electronic flow is favored from the substituents to the fullerene due to the availability of its low energy LUMO. This last characteristic is supported by the reactivity indexes which also show that these species are the ones with maximum electron flow, therefore it is expected that **APF** will be a good semiconductor and **BCF** perhaps can be classified as a synthetic metal.

5. Conclusions

Several organic and organometallic derivatives of fullerene were studied from a theoretical point of view. Firstly, **PF** which is a known substance yields interesting results. The molecule is a much more effective semiconductor species than fullerene alone, but curiously the effect arose from the renewed participation of resonance electronic flow in the fullerene without any participation on the part of the new ring in the frontier molecular orbitals. In order to clarify this point, new calculations were carried out on some derivatives for which the inductive effect was taken into account. Thus, the nitro and the amino derivatives were also considered and it was evident that the electron withdrawal substituent ($-NO_2$) had no major influence on the entire molecule because its behavior was very similar to that observed in **PF**. However, the electron releasing group ($-NH_2$) caused significant changes. In this

case there was participation of the entire aromatic ring on the frontier molecular orbitals and this represents the best semiconductor compound. The complex arising from the combination of **F** and **BC** has very interesting characteristics: the frontier molecular orbitals seem to be completely independent of each other, the HOMO is completely localized on the organometallic substituent, whereas the LUMO belongs completely to the **F**. Likewise, this last molecule also shows synthetic metal behavior.

Acknowledgments

The authors want to acknowledge Joaquín Morales, Oralia Jiménez y Ma. Teresa Vázquez for technical help.

References

[1] R. Taylor, The Chemistry of Fullerenes, World Scientific, Singapore, 1995.
[2] F. Wudl, A. Hirsch, K.C. Khemani, T. Suzuki, P.M. Allemand, A. Koch, H. Eckert, G. Srdanov, H. Webb, Fullerenes: Synthesis, Properties and Chemistry of Large Carbon Clusters, in: G.S. Hammond, V.S. Kuck (Eds), Washington, 1992.
[3] A. Hirsch, T. Grösser, A. Skiebe, A. Soi, Synthesis of isomerically pure organohydrofullerenes, Chem. Ber. 126 (1993) 1061–1067.
[4] A. Hirsch, A. Soi, H.R. Karfunkel, Titration of C_{60}: a method for the synthesis of organofullerenes, Angew. Chem. In. Ed. Engl. 31 (1992) 766–768.
[5] G.A. Olah, I. Bucsi, R. Aniszfeld, G.K. Surya-Prakash, Chemical reactivity and functionalization of C60 and C70 fullerenes, Carbon 30 (1992) 1203–1211.
[6] A.D. Becke, Density-functional exchange-energy approximation with correct asymptotic behavior, Phys. Rev. A 38 (1988) 3098–3100.
[7] J.P. Perdew, Y. Wang, Accurate and simple analytic representation of the electron-gas correlation energy, Phys. Rev. B 45 (1992) 13244–13249.
[8] Gaussian 09, Revision A.1, M.J. Frisch, G.W. Trucks, H.B. Schlegel, G.E. Scuseria, M.A. Robb, J.R. Cheeseman, G. Scalmani, V. Barone, B. Mennucci, G.A. Petersson, H. Nakatsuji, M. Caricato, X. Li, H.P. Hratchian, A.F. Izmaylov, J. Bloino, G. Zheng, J.L. Sonnenberg, M. Hada, M. Ehara, K. Toyota, R. Fukuda, J. Hasegawa, M. Ishida, T. Nakajima, Y. Honda, O. Kitao, H. Nakai, T. Vreven, J.A. Montgomery, Jr., J.E. Peralta, F. Ogliaro, M. Bearpark, J.J. Heyd, E. Brothers, K.N. Kudin, V.N. Staroverov, R. Kobayashi, J. Normand, K. Raghavachari, A. Rendell, J.C. Burant, S.S. Iyengar, J. Tomasi, M. Cossi, N. Rega, J.M. Millam, M. Klene, J.E. Knox, J.B. Cross, V. Bakken, C. Adamo, J. Jaramillo, R. Gomperts, R.E. Stratmann, O. Yazyev, A.J. Austin, R. Cammi, C. Pomelli, J.W. Ochterski, R.L. Martin, K. Morokuma, V.G. Zakrzewski, G.A. Voth, P. Salvador, J.J. Dannenberg, S. Dapprich, A.D. Daniels, Ö. Farkas, J.B. Foresman, J.V. Ortiz, J. Cioslowski, D.J. Fox, Gaussian, Inc., Wallingford CT, 2009.
[9] B.J. Delley, An all electron numerical method for solving the local density functional for polyatomic molecules, Chem. Phys. 92 (1990) 508–517.
[10] B.J. Delley, From molecules to solids with the DMol3 approach, Chem. Phys. 113 (2000) 7756–7764.
[11] J.P. Perdew, Y. Wang, Accurate and simple analytic representation of the electron-gas correlation energy, Phys. Rev. B 45 (1992) 13244–13249.
[12] M. Dolg, U. Wedig, H. Stoll, H. Preuss, Energy-adjusted ab initio pseudopotentials for the first row transition elements, Chem. Phys. 86 (1987) 866–872.
[13] A. Bergner, M. Dolg, W. Kuechle, H. Stoll, H. Preuss, Ab initio energy-adjusted pseudopotentials for elements of groups 13–17, Mol. Phys. 80 (1993) 1431–1441.
[14] T.M. Krygowski, Crystallo-graphic studies of inter and intramolecular interactions reflected in aromatic character of π-electron systems, Chem. Inf. Comput. Sci. 33 (1993) 70–78.
[15] T.M. Krygowski, M.K. Cyranski, Structural aspects of aromaticity, Chem. Rev. 101 (2001) 1385–1419.
[16] R.G. Parr, L.V. Szentpály, S. Liu, Electrophilicity index, J. Am. Chem. Soc. 121 (1999) 1922–1924.
[17] R. Salcedo, Fullerenocene, Polyhedron 28 (2009) 431–436.